NASA CONTRACTOR REPORT

ENTRY LENGTH FOR THE ROCKET METEOROLOGICAL RADIATION SHIELD

by Forrest L. Staffanson, Sadiq Alsaji, and Ronald Fazzio

Prepared by
UNIVERSITY OF UTAH
Salt Lake City, Utah
for

NATIONAL AERONAUTICS AND SPACE ADMINISTRATION • WASHINGTON, D. C. • OCTOBER 1968

ENTRY LENGTH FOR THE ROCKET METEOROLOGICAL RADIATION SHIELD

By Forrest L. Staffanson, Sadiq Alsaji, and Ronald Fazzio

Prepared under Grant No. NGR-45-003-025 by
~~UNIVERSITY OF~~ UTAH
Salt Lake City, Utah

for

NATIONAL AERONAUTICS AND SPACE ADMINISTRATION

For sale by the Clearinghouse for Federal Scientific and Technical Information
Springfield, Virginia 22151 – CFSTI price $3.00

ABSTRACT

A derivation is presented for the thermal entry length which determines the depth within a tubular radiation shield that a temperature sensor may be placed without incurring convective heat transfer between the shield and sensor. Data are presented as a function of shield diameter, altitude, and sensor viewing angle. It is concluded that radiation shields of the diameter of the 4-inch meteorological rocket will provide significant shielding to 80 km altitude and shields of the diameter of the 1-inch dart to 60 km.

INTRODUCTION

Meteorological rocketsondes commonly use a thermistor as the atmospheric temperature sensing element. The thermistor is mounted in such a way as to be immersed in the air forward of the sonde as it descends through the upper atmosphere on a parachute. The low density of the air at the higher altitudes decreases the thermometric sensitivity of the thermistor so that radiation errors become large. The accuracy of radiation corrections for a given flight is limited by the uncertainty or variability of the radiation environment during the flight. The suggestion arises then of a radiation shield which, in effect, replaces all or part of the less desirable radiation environment with one which is less intense, more uniform or predictable, measurable, or otherwise permits more accurate correction of the sensor data. Obviously the effect of the shield on the air flow over the thermistor must be considered in order to achieve the desired result.

Perhaps the simplest approach to shielding is that of placing an opaque wall around the thermistor in such a way as to maximize the solid angle of the replaced radiation environment without influencing the temperature of the air stream at the thermistor. The air temperature at the thermistor surface may be influenced by the presence of the shield through hydrodynamic (acceleration) effects and thermal (heating) effects induced by the wall on the air flow. These effects

may be utilized to advantage in some shielded sensor concepts. The present discussion, however, will be concerned with the simpler concept in which the thermistor is placed in the entrance region of a cylindrical tube deep enough to maximize shielding but not deep enough to encounter the thermal boundary layer nor the hydrodynamic boundary layer existing in the entrance region of the tube.

BASIC EQUATION AND INPUTS

The shapes of the thermal and hydrodynamic boundary layers in the entrance region of a tube are exemplified in Fig. 1 by those of laminar continuum flow. The temperature and velocity distributions are shown, and as the figure illustrates, the thickness, δ_T, of the thermal boundary layer increases faster than that, δ, of the hydrodynamic boundary layer. This occurs for fluids with Prandtl number[1] less than unity. This being the case, the thermal entry length Le_T is less than the hydrodynamic entry length Le. Le_T is, therefore, the parameter of interest for locating the sensor within the shield.

The flow in tubes is always laminar if the Reynolds number is less than some critical value. A Reynolds number which is less than 2300, based on the mean velocity and tube diameter, is assurance of laminar flow. If the entering fluid is especially free of previous disturbances and if the tube walls are smooth, the critical Reynolds number may be ten times this value or more. [Schlicting 1960.] It is supposed that the atmosphere encountered by the descending sonde is quite free of small-scale disturbances (at least when compared to air flows from wind tunnel blowers) and, therefore, that the critical Reynolds number is larger than 2300.

---

[1] $$Pr = \frac{\mu c_p}{k} = \left(\frac{\mu}{\rho}\right)\Big/\left(\frac{k}{\rho c_p}\right) = \frac{\text{"momentum diffusivity"}}{\text{"thermal diffusivity"}} = \frac{\delta}{\delta_T} = \frac{Le_T}{Le} = 0.72 \text{ for air.}$$

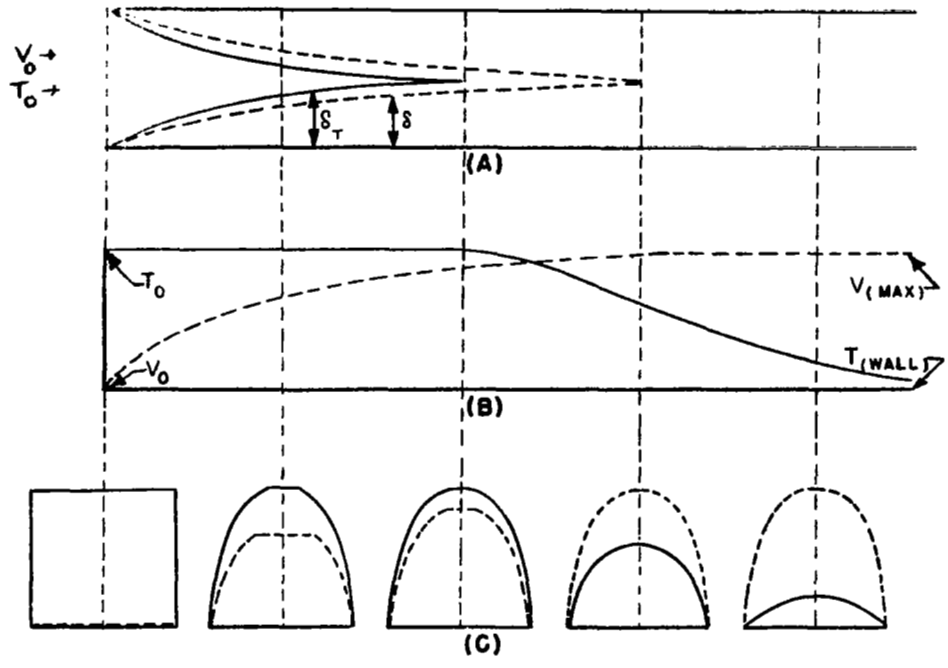

Fig. 1. Illustration of the temperature and velocity distribution in the entrance region of a tube, showing:

A. Thermal and hydrodynamic boundary layer profiles

B. Centerline temperature and velocity

C. Successive cross sections of the temperature and velocity distributions.

Even in the event that turbulent flow occurs in the tube, the boundary layer is always laminar at the leading edge and continues to be laminar downstream to a point where the local Reynolds number reaches a critical value. At the point of transition to turbulent flow, the boundary layer becomes much more thick. A transition criterion indicative of the point of commencement of turbulent flow is suggested by Kays [1966].

$$\left(Re_{\delta}\right)_{CRITICAL} = 360$$

Here the Reynolds number is based on the local centerline velocity and on the momentum thickness. The corresponding depth into the tube might be considered for use as the entry length if turbulence were expected to occur. The cases under discussion are sufficiently clear of turbulent conditions so laminar conditions are assumed for the remainder of the discussion.

Shields of regular polygonal[2] cross section are considered

---

[2] Entry lengths for rectangular cylinders range for varying ratios of their sides from Le for the square (d_h = side) to Le for parallel plates (d_h = twice the separation distance) [Hartmett, 1962].

in this discussion as hydrodynamically equivalent to a circular tube having diameter equal to the hydraulic diameter d_h.

$$d_h = 4 \frac{\text{(cross sectional area)}}{\text{(perimeter)}} \tag{1}$$

Thus the entry length, Le, of a square cylinder of side d is equal to that of a circular cylinder of diameter d.

Kays [1966] approximates the thermal entry length for circular tubes in laminar flow as

$$Le_T \approx 0.05 \text{ d Re Pr} = 0.036 \text{ d Re} \tag{2}$$

$$Re = \frac{\rho V d}{\mu}$$

Minor variations occur between authors partly due to differing definitions for the commencement of fully developed flow. Calculations cited by Eckert and Drake [1959] give

$$Le_T = 0.0288 \text{ d Re} \tag{3}$$

which agrees exactly with results from Schlicting [1960] for the hydrodynamic entry length in a square tube,

$$Le = 0.04 \text{ d Re} \tag{4}$$

$$Le_T = Le\ Pr = 0.0288\ d\ Re$$

The latter expression is used in this paper for the thermal entry length of the shield under conditions of continuum flow.

At the lower altitudes of interest the air stream through a cylindrical shield behaves as a continuum. At higher altitudes the air density becomes sufficiently low that rarefaction effects appear in the boundary layer and the expressions for entry length must be modified to agree with experimental results. According to Schaaf and Chambre [1961] deviation from continuum flow is observed when

$$0.01 < \frac{M}{Re}\ , \qquad Re < 1 \qquad (5)$$

$$0.01 < \frac{M}{\sqrt{Re}}\ , \qquad Re > 1 \qquad (6)$$

referring Knudsen number to the body dimension for $Re < 1$ and to boundary layer thickness for $Re > 1$. Some experimentalists suggest, however, that onset of rarefaction effects in tubes is not so easily predicted [Carley, 1965].

Rarefied flow in the entrance region of circular cylinders was studied analytically by Hanks [1963]. Adapting the results of his analysis of incompressible flow under slip conditions at the boundaries gives

$$Le_T = C\ d\ Re \qquad (7)$$

for the thermal entry length where the coefficient C depends on Knudsen number referred to the shield diameter.

$$Kn = \frac{\lambda}{d} = \frac{\text{atmospheric mean free path}}{\text{tube diameter}}$$

Table 1 and Fig. 2 give C(Kn) according to Hanks. Additional computation was necessary to supplement the values tabulated by Hanks. No explanation nor evaluation is attempted here concerning the maximum or other behavior of the function.

TABLE I

Entry Length Coefficient, C, for Rarefied Flow

Kn	C
0	0.0288
0.00100	0.0288
0.00500	0.0295
0.0100	0.0302
0.0500	0.0335
0.0556	0.0338
0.0625	0.0342
0.0714	0.0346
0.0833	0.0350
0.100	0.0354
0.125	0.0358
0.1667	0.0360
0.250	0.0357
0.500	0.0329

Though a fully acceptable theory for rarefied entrance flow does not yet exist [Carley and Smetana, 1966], a reasonable degree of agreement with Hanks results is found in the treatment by Sparrow [1962] and

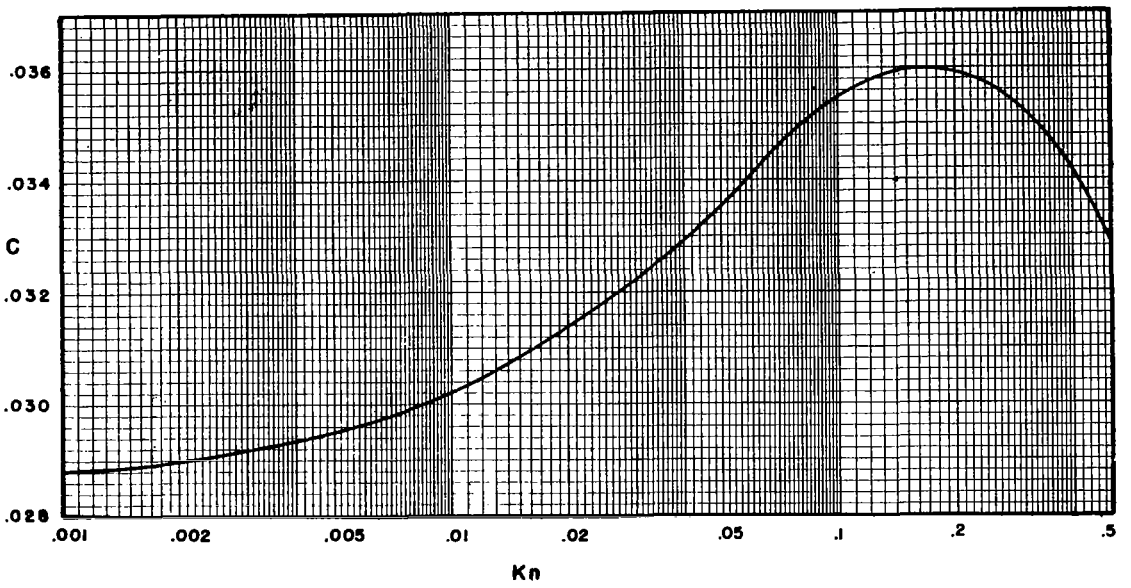

Fig. 2. Thermal entry length coefficient [after Hanks, [1963].

in the experimental results reported by Carley [1965] of two-dimensional rarefied flow between parallel plates. Notice that Hanks expression when Knudsen number is small coincides with Eq. 3 adopted above for continuum flow. Values for C are taken from Fig. 2 for the purposes of this report.

Representative air speeds for rocketsondes are tabulated in Table II and plotted in Fig. 3. The middle air speed profile m/A = 0.02

TABLE II

Air Speed, V (m/sec)

m/A (kg/m^2)	0.03	0.02	0.01
Z (km)			
80	300	300	300
75	332	299	234
70	309	258	177
65	231	179	120
60	156	122	84
55	108	86	61
50	76	62	43
45	54	43	34
40	37	32	--

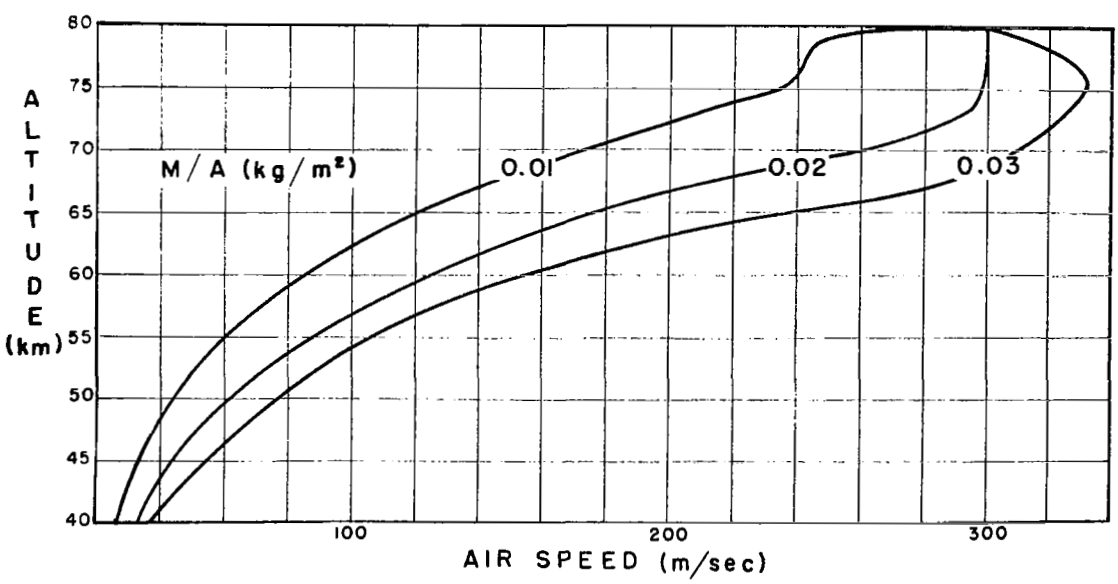

Fig. 3. Representative rocketsonde air speed profiles.

is nominally that of a calculated two-dimensional trajectory using a variable drag coefficient [Eddy, 1965] typical of the standard ARCAS type sonde-parachute system. In addition, a faster falling and a slower falling parachute are included. The two other air speed profiles correspond to a 50 percent variation in parachute mass to reference area ratio, $m/A = 0.02 \pm 0.01$. The high speed curve, $m/A = 0.03$, approximates the performance of systems commonly used in rocket darts and gun probes, while the low speed curve $m/A = 0.01$ represents possible future parachute systems. Thermodynamic properties of the air remote from the shield are taken from the U. S. Standard Atmosphere, 1962. Pertinent values are listed in Table III.

TABLE III

Standard Atmosphere

Z (km)	C_s (m/sec)	$\frac{\mu}{\rho}\left(m^2\ sec^{-1}\right)$	λ (cm)
90	269.44	3.84	2.56
85	269.44	1.53	1.02
80	269.44	0.609	0.407
75	283.61	0.307	0.187
70	297.14	0.164	0.0928
65	310.10	0.926	0.0488
60	320.61	0.0532	0.0266
55	326.70	0.0299	0.0145
50	329.80	0.0166	0.00791
45	325.82	0.00850	0.00413
40	317.19	0.00401	0.00203
35	308.30	0.00181	0.000960
30	301.71	0.000801	0.000441

RESULTS

Shield diameters of 1 and 10 cm were selected for a preliminary tabulation. Tables IV and V give the values of thermal entry length versus altitude for the two shield sizes and three air speeds. Values of the associated dimensionless parameters Re, $M/\sqrt{Re}$, Kn, and C are listed for reference. All values of Re are well below the critical value of 2300 so calculations based on laminar flow conditions are certainly valid. Curves of Le_T vs. Z are given in Figs. 4 and 5.

Comparison of Le_T for the two shield sizes clearly shows its dependence on d^2 according to

$$Le_T = C\ d\ Re = C\ d^2\ \rho V/\mu$$

Larger shield diameters, therefore, provide a measure against the eventually overruling effect of the exponentially decreasing air density. The linear dependence on air speed is also seen, that is, within the smaller effects of the remaining factors.

These results indicate that, as altitude increases, thermal entry length decreases. For a 1 cm diameter shield, thermal entry length decreases from about 2.7 cm at 40 km, for the high-speed parachute, to a trivial 0.17 cm at 80 km. The corresponding values for a 10 cm shield are 2.6 meters to a more acceptable high altitude value of 16 cm. Since the sensor must remain forward of the entry

TABLE IV

Entry Length Parameters for 1 cm Diameter Shield

Z (km)	Re	$M/\sqrt{Re}$	Kn	C	Le_T (cm)
		$m/A = .03\ kg/m^2$ d = 1 cm			
80	4.93	.501	.407	.0343	.169
75	10.5	.350	.187	.0360	.378
70	18.8	.240	.0928	.0352	.663
65	24.9	.149	.0488	.0337	.840
60	29.3	.0898	.0266	.0323	.945
55	36.0	.0549	.0145	.0310	1.12
50	45.7	.0340	.00791	.0298	1.36
45	63.0	.0270	.00413	.0293	1.84
40	92.2	.0121	.00203	.0290	2.67
		$m/A = .02\ kg/m^2$ d = 1 cm			
80	4.93	.501	.407	.0343	.169
75	9.75	.338	.187	.0360	.351
70	15.7	.219	.0928	.0352	.553
65	19.4	.131	.0488	.0337	.653
60	23.0	.0796	.0266	.0323	.743
55	28.9	.0492	.0145	.0310	.895
50	37.4	.0378	.00791	.0298	1.12
45	51.1	.0186	.00413	.0293	1.50
40	80.5	.0113	.00203	.0290	2.34
		$m/A = .01\ kg/m^2$ d = 1 cm			
80	4.93	.501	.407	.0343	.169
75	7.64	.299	.187	.0360	.277
70	10.79	.182	.0928	.0352	.380
65	12.91	.107	.0488	.0337	.435
60	15.84	.0661	.0266	.0323	.512
55	20.21	.0412	.0145	.0310	.627
50	26.06	.0257	.00791	.0298	.777
45	39.53	.0164	.00413	.0293	.116
40	-----	-----	.00203	.0290	----

TABLE V

Entry Length Parameters for 10 cm Diameter Shield

Z (km)	Re	$M/\sqrt{Re}$	Kn	C	L_{eT} (cm)
m/A = .03 d = 10 cm					
80	49.3	.159	.0407	.0333	16.4
75	105.0	.111	.0187	.0316	33.2
70	188.0	.0759	.00928	.0305	56.5
65	249.0	.0471	.00488	.0295	73.5
60	293.0	.0284	.00266	.0291	85.2
55	360.0	.0174	.00145	.0288	104.0
50	457.0	.0108	.000791	.0288	132.0
45	630.0	.00655	.000413	.0288	181.0
40	922.0	.00384	.000203	.0288	266.0
m/A = .02 d = 10 cm					
80	49.3	.159	.0407	.0333	16.4
75	97.5	.107	.0187	.0316	30.8
70	157.0	.0693	.00928	.0305	47.2
65	194.0	.0416	.00488	.0295	57.2
60	230.0	.0252	.00256	.0291	66.9
55	289.0	.0156	.00145	.0288	83.1
50	374.0	.00973	.000791	.0288	107.8
45	511.0	.00590	.000413	.0288	147.0
40	805.0	.00358	.000203	.0288	232.0
m/A = .01 d = 10 cm					
80	49.3	.159	.0407	.0333	16.4
75	76.4	.0945	.0187	.0316	24.1
70	108.0	.0574	.00928	.0305	32.4
65	129.0	.0339	.00488	.0295	38.1
60	158.0	.0209	.00256	.0291	46.1
55	202.0	.0130	.00145	.0288	58.2
50	261.0	.00812	.000791	.0288	75.0
45	395.0	.00519	.000413	.0288	114.0
40	-----	------	.000203	.0288	-----

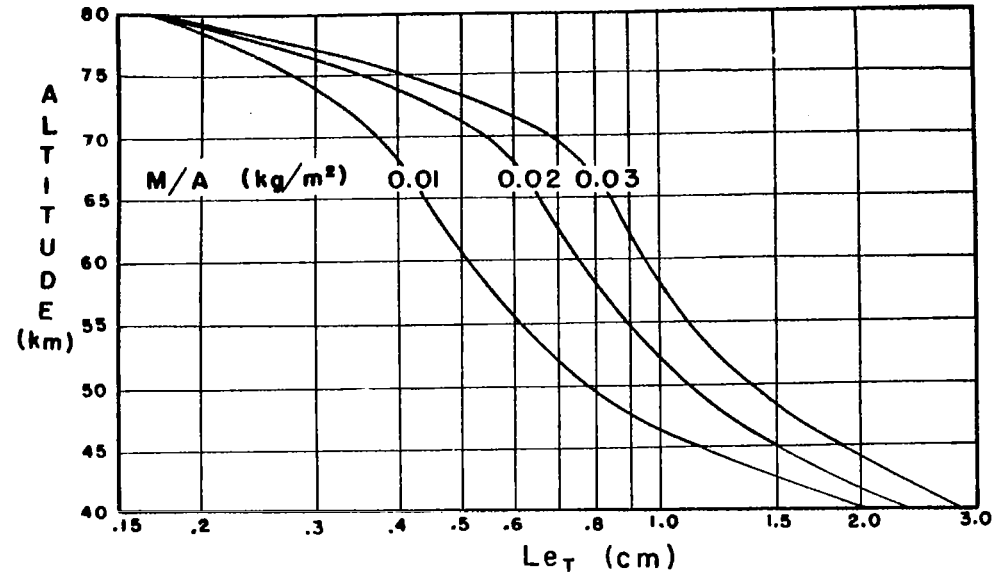

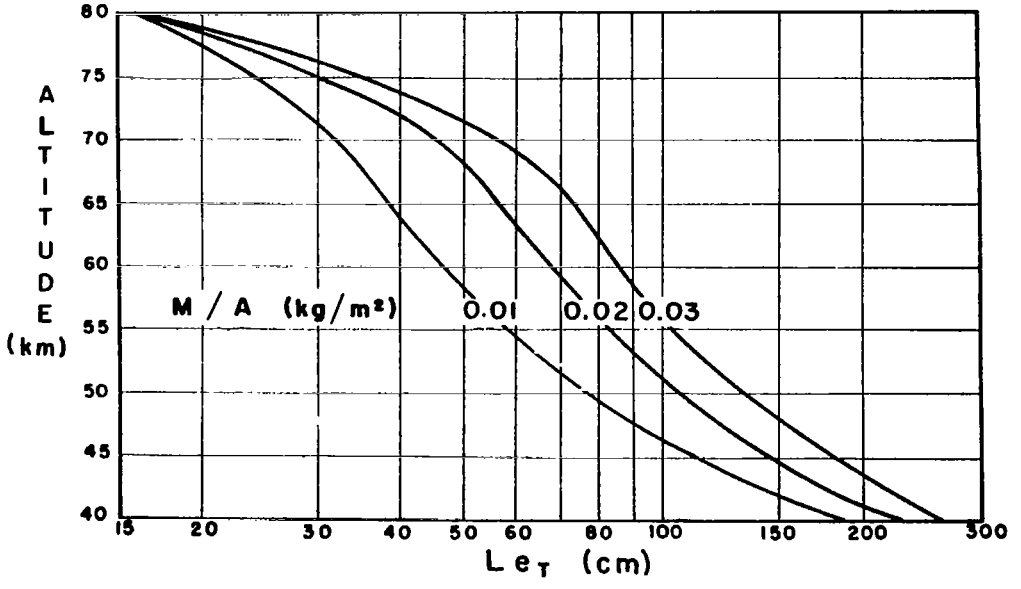

Figs. 4 and 5. Thermal entry for 1 cm (upper) and 10 cm (lower) diameter shields.

length, necessary exposure to the external environment increases with altitude and shielding becomes less effective.

It must be kept in mind that the entry lengths calculated are theoretical maxima for the location of the sensor. In order to avoid contact with the thermal boundary layer under real conditions, a safety margin must be ascertained based on the size of the sensor, including the conductively near region of its support, and on probable departures from the ideal conditions of steady flow. Suppose that adequate shielding requires a maximum view half-angle of θ and a reasonable safety margin requires the sensor to be placed at $\alpha Le_T < Le_T$; then the sensor depth S is limited by

$$\frac{d}{2 \tan \theta} < S < \alpha \, Le_T$$

where θ is illustrated in Fig. 6. It follows that

$$Le_T > \frac{d}{2\alpha \tan \theta}$$

which implies a minimum shield diameter

$$d = \frac{\mu}{2\alpha C \rho V \tan \theta}$$

On the other hand, given a shield diameter d, a specified view half angle θ, and a safety factor α, the minimum entry length is defined by

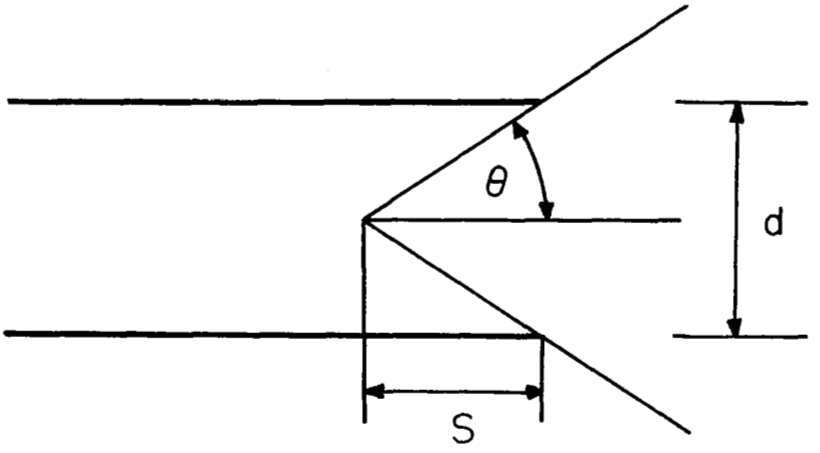

Fig. 6. View half-angle θ of a sensor placed at depth S in shield of diameter d.

$$\left(Le_T\right)_o = \frac{d}{2\alpha \tan \theta}$$

Table VII lists values of $\left(Le_T\right)_o$ for selected values of d, α, and θ. Table VI lists entry lengths corresponding to these diameters over the altitude range 40-80 km using the nominal (m/A = 0.02) parachute speeds. Thus, the maximum altitude associated with a given set of values d', θ', and α' is that altitude in Table VI corresponding to $Le_T = \left(Le_T\right)_o'$ and d = d'. Cross plots of the two tables are given in Fig. 7.

TABLE VI

Entry Length Le_T (cm) vs.

Altitude (km) and Shield Diameter (cm)

d(cm)	1	2	3	5	7	10	15
Z(km)							
80	0.169	0.708	1.59	4.30	8.21	16.4	35.6
75	0.351	1.37	3.01	8.01	15.4	30.8	67.1
70	0.553	2.10	4.58	12.3	23.7	47.2	105.
65	0.653	2.47	5.41	14.6	28.3	57.2	128.
60	0.743	2.82	6.22	17.0	33.1	66.9	150.
55	0.895	3.46	7.66	21.1	41.1	83.1	187.
50	1.12	4.40	9.80	27.1	52.9	107.8	243.
45	1.50	5.93	13.3	36.8	72.1	147.	331.
40	2.34	9.28	20.9	58.0	114.	232.	522.

It is noted that the sensor requires some finite diameter of the entry core, and that the core diameter is asymptotically small in the deeper part of the entry region (Fig. 1(A)). The resulting requirement for a small value of α may be relaxed perhaps with the use of diverging or vented shield walls which tend to draw the boundary layer away from the shield axis. To what extent these aspects modify the conclusions of this discussion is left to subsequent studies of specific shield designs.

TABLE VII

Minimum Entry Length $\left(Le_T\right)_o$ (cm), vs. Shield Diameter d(cm), View Half-Angle θ(deg), and Safety Factor α.

d(cm)	1	2	3	5	7	10	15
θ(°)	α = 0.3						
10	9.45	18.9	28.4	47.3	66.2	94.5	142.
20	4.58	9.16	13.7	22.9	32.1	45.8	68.7
30	2.89	5.77	8.66	14.4	20.2	28.9	43.3
40	1.99	3.97	5.96	9.93	13.9	19.9	29.8
50	1.40	2.80	4.20	7.00	9.79	14.0	21.0
	α = 0.5						
10	5.67	11.3	17.0	28.4	39.7	56.7	85.1
20	2.75	5.50	8.24	13.7	19.2	27.5	41.2
30	1.73	3.46	5.20	8.66	12.1	17.3	26.0
40	1.19	2.38	3.58	5.96	8.34	11.9	17.9
50	0.839	1.68	2.52	4.20	5.87	8.40	12.6
	α = 0.7						
10	4.05	8.10	12.2	20.3	28.4	40.5	60.8
20	1.96	3.93	5.89	9.81	13.7	19.6	29.4
30	1.24	2.47	3.71	6.19	8.66	12.4	18.6
40	0.851	1.70	2.55	4.26	5.96	8.51	12.8
50	0.599	1.20	1.80	3.00	4.20	5.99	8.99
	α = 1.0						
10	2.84	5.67	8.51	14.2	19.8	28.4	42.5
20	1.37	2.75	4.12	6.87	9.62	13.7	20.6
30	0.866	1.73	2.60	4.33	6.06	8.66	13.0
40	0.596	1.19	1.79	2.98	4.17	5.96	8.94
50	0.420	0.839	1.26	2.10	2.94	4.20	6.29

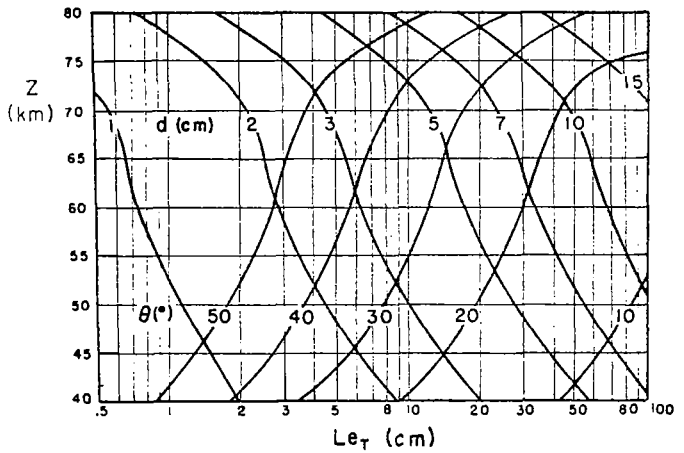

α = 0.3

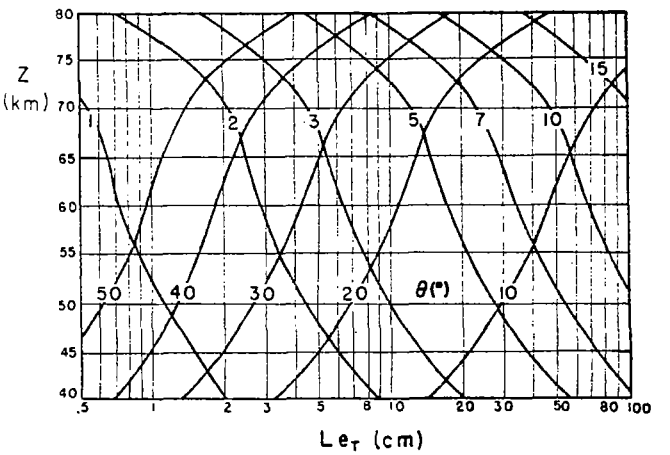

α = 0.5

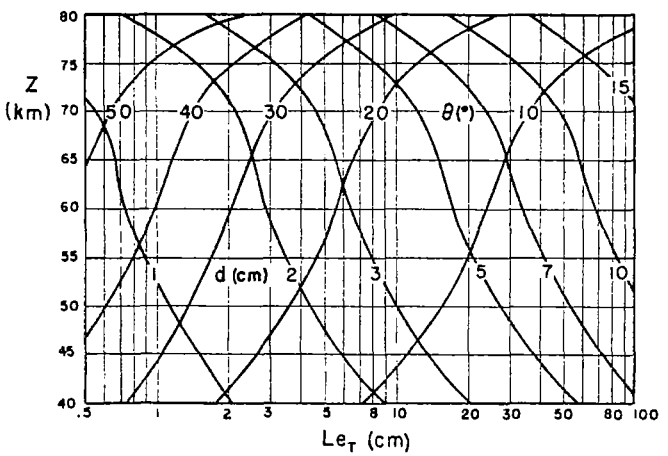

α = 0.7

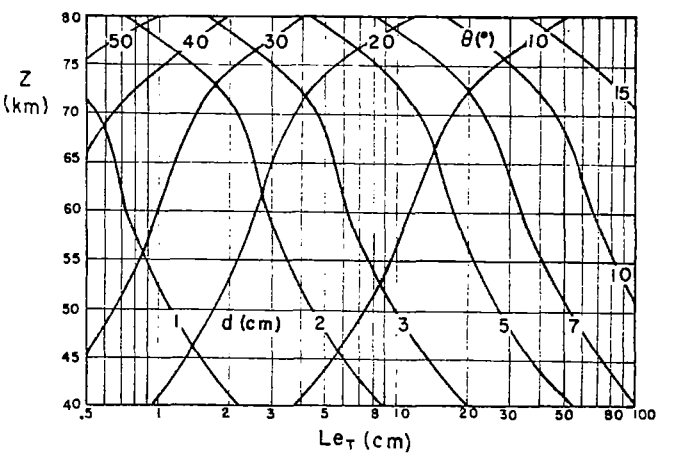

α = 1.0

Fig. 7. Cross plots of data from Tables VI and VII, relating limiting values of shield diameter d, altitude z, view half-angle θ, and thermal entry length Le_T for safety factors α.

CONCLUSION

Data are presented which relate the thermal entry length of a cylindrical tube to its diameter and altitude, based on Hanks' analysis of rarefied incompressible flow and on nominal air speed profiles of rocket meteorological parachute systems. Tabulated data and curves further relate the radiation shield diameter, sensor view angle, and sensor shield depth relative to entry length. Thus, maximum altitudes are calculable for given specifications of shield size and view factor.

In order to avoid the thermal boundary layer inside a cylindrical radiation shield, the air temperature sensing element must be placed forward of the thermal entry length. Thermal entry length decreases with altitude so that the sensor's exposure to external radiation must increase for operation at higher altitudes (where shielding is most needed). On the other hand, increased shield diameters increase thermal entry length and allow deeper placement of the sensor for greater shielding. Though boundary layer techniques in the shield conceivably could modify these conclusions, it is expected that shield dimensions of the size of conventional four-inch meteorological rocket nose cones permit shielding to about 80 km altitude, and of the size of one-inch darts to about 60 km. This presumes a practical maximum view half angle of about 30° and a safety factor of about 0.5.

LIST OF SYMBOLS

A	parachute reference area
C	entry length factor
cp	specific heat of air at constant pressure
C_s	speed of sound
d	shield diameter
d_h	hydraulic diameter
k	thermal conductivity of the air
K_n	Knudsen number
Le	hydrodynamic entry length
Le_T	thermal entry length
M	Mach number
m	mass of parachute system
Re	Reynolds number
S	sensor depth into shield
Pr	Prandtl number
V	air speed
Z	geometric altitude
α	equals S/Le_T, safety factor
δ	hydrodynamic boundary layer thickness
δ_T	thermal boundary layer thickness
λ	mean free path
ρ	air density
μ	coefficient of viscosity
θ	half angle of sensor view

REFERENCES

Carley, C. T. Jr., "Rarefied Gas Flow in a Short Tube," Ph.D. Thesis, North Carolina State University, Raleigh, North Carolina, 1964.

Carley, C. T. Jr., and F. O. Smetana, "Experiments on Transition Regime Flow Through a Short Tube with a Bellmouth Entry," J. Amer. Inst. Astronautics and Aeronautics, Vol. 4, No. 1, January, 1966, p. 47.

Eddy, Amos, C. E. Duchon, F. M. Haase, D. R. Haragan, "Determination of Winds from Meteorological Rocketsondes," Report No. 2, under Contract DA-23-072-AMC-1564, Atmospheric Science Group, College of Engineering, University of Texas, Austin, Texas, November, 1965.

Eckert, E. R. G., and Robert M. Drake, Jr., Heat and Mass Transfer, Second Edition, McGraw-Hill Book Company, New York, June, 1962, p. 154.

Hanks, R. W., "Velocity Profile Development in the Entrance Region of a Right Circular Cylinder with Slip at the Walls," The Physics of Fluids, Vol. 6, No. 11, November, 1963, p. 1645.

Hartmett, J. P., G. C. Y. Koh, and S. T. McComas, Transactions of the American Society of Mechanical Engineers, Vol. 84, 1962, pp. 82-88.

Kays, W. M., Convective Heat and Mass Transfer, McGraw-Hill Book Company, New York, 1966, pp. 125-144.

Schaaf, S. A. and P. L. Chambre, Flow of Rarefied Gases, Princeton University Press, New Jersey, 1961, p. 5.

Schlicting, Hermann, Boundary Layer Theory, Fourth Edition, McGraw-Hill Book Company, New York, 1960, pp. 376, 171.

Sparrow, E. M., T. S. Lundgren, and S. H. Lin, "Slip Flow in the Entrance Region of a Parallel Plate Channel," Proceedings of 1962 Heat and Transfer and Fluids Mechanics Institute, Stanford University Press, 1962, pp. 223-238.